2004 RISP International Workshop on Nonlinear
Circuit and Signal Processing (NCSP'04)
Hawaii, USA, Mar. 5-7, 2004.

On Two Types of Network Topologies of Small-World Cellular Neural Networks

Kazuya TSURUTA, Zonghuang YANG, Yoshifumi NISHIO and Akio USHIDA

Tokushima University
2-1 Minami-Josanjima, Tokushima, Japan
Phone:+81-88-656-7470
FAX:+81-88-656-7471
Email: tsuruta@ee.tokushima-u.ac.jp

1. Introduction

Studies of network map are very important, because they help us to understand the basic features and requirements of various systems. So far many connection topologies of network assumed to be either completely regular or completely random have been studied in the past. Cellular Neural Network (CNN) model invented by Chua and Yang in 1988 [1] is a typical of those completely local connectivities, which is presented as a preferred implementation of locally and regularly coupled neural networks. The CNN has been successfully used for various high-speed parallel signals processing applications such as image processing, pattern recognition as well as modeling of various phenomena in nonlinear systems [1]-[4]. However, in many cases in real life, many network topologies such as biological, technological and social networks are known to be not completely random nor completely local but somewhere in between. This was modeled in an interesting work by Watts and Strogatz in 1998 [5] as the small-world model. The model is a network consisting of many local links and fewer long range 'short cuts'. Therefore, it has a high clustering coefficient like regular lattices and a short characteristic path length of typical random networks. Interesting examples are shown by collaboration of movie stars, connectivity of internet web pages or neural nets, etc.

Recently, the authors have proposed Small-World Cellular Neural Network (SWCNN) [6], which is constructed by introducing some random couplings between cells of the original Chua-Yang CNN. In [6] we have reported some basic results using the concept of SWCNN. In this article, we propose two types of network topologies of the SWCNN and investigate the features of the two SWCNNs.

2. Network Topologies of SWCNN

In this section, we describe the two types of the connection topology of the SWCNN composed of a two-dimensional M by N array structure.

2.1. Added SWCNN

The first network topology is named as "Added SWCNN", which is the same topology as SWCNN in [6].

The Added SWCNN is obtained by just adding some random couplings between cells in the original Chua-Yang CNN. We introduce a probability p_c, which means what percentage of the cells in the CNN occur to random coupling to another cell. We assume that, besides its local couplings, each cell in the array is only permitted a maximum of one random coupling to another cell. Thereby, for a $M \times N$ array, it has a maximum p_c of $M \times N/2$ pairs of cell couplings. Figure 1 shows a sketch map of the SWCNN consisting of 4×4 cells. Obviously, when $p_c = 0$, the SWCNN is completely the same with the original CNNs, and the maps correponding to $0 < p_c < 1$ and $p_c = 1$ are respectively shown in the middle part and the right hand side of Fig. 1.

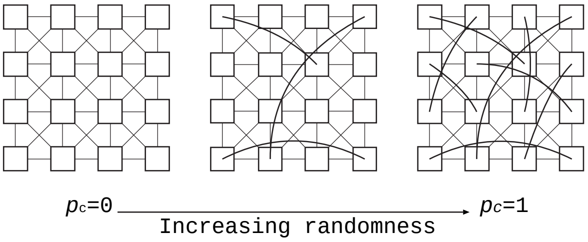

Figure 1: Added SWCNN architecture.

The state equation of each cell $c(i,j)$ of the SWCNN is formulated by Eq. (1), and the output equation is defined by Eq. (2).

$$\begin{aligned}\dot{x}_{ij}(t) = &-x_{ij}(t) + I \\ &+ \sum_{c(k,l)\in N_r(i,j)} A(i,j;k,l)y_{kl}(t) \\ &+ \sum_{c(k,l)\in N_r(i,j)} B(i,j;k,l)u_{kl}(t) \\ &+ w_c M(i,j;p,q)y_{pq}(t)\end{aligned} \tag{1}$$

$$y_{ij}(t) = \frac{1}{2}(|x_{ij}(t)+1| - |x_{ij}(t)-1|) \tag{2}$$

$$i = 1,2,...,M, \quad j = 1,2,...,N.$$

where $N_r(i,j)$ denotes the neighbor cells of radius r of a cell $c(i,j)$; A, B, and I are real constants called as feedback template, control template and bias current, respectively; x_{ij}, y_{ij}, u_{ij} denotes the state, input and output of the cell, respectively; $M(i,j;p,q)$ describes the small-world map that is randomly created by program with indicating the probability p_c in advance, if there is a coupling between one cell $c(i,j)$ and another cell $c(p,q)$, then the $M(i,j;p,q)$ is equal to 1, otherwise is zero; and w_c stands for the coupling weight between the randomly coupled cells.

In order to investigate the features of the network, we calculated the characteristic path length L(p_c) and the clustering coefficient C(p_c) as varying p_c. The characteristic path length L(p_c) is defined as the number of edges in the shortest path between two vertices, averaged over all pairs of vertices [5]. The clustering coefficient C(p_c) is defined as follows; Suppose that a vertex v has k_v neighbours; then at most $k_v(k_v-1)/2$ edges can exist between them. Let C_v denote that fraction of these allowable edges that actually exist. Define C(p_c) as the average of C_v over all v [5].

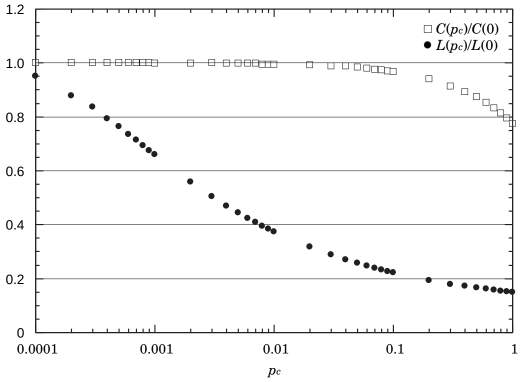

Figure 2: Characteristic path length and clustering coefficient of Added SWCNN.

The results are shown in Fig. 2. Because we make a restriction such that one cell has at most one random coupling, the clustering coefficient does not approach zero even if p_c becomes 1.0. However, the characteristic path length becomes shorter and the network possesses the feature of the small-world networks.

2.2. Rewired SWCNN

The second network topology is named as “Rewired SWCNN”.

The Rewired SWCNN is obtained by rewiring some couplings between cells in the original Chua-Yang CNN. Namely, we choose a cell and a coupling that connects it to its nearest neighbour. We reconnect this coupling to another cell chosen at random over the whole network. We repeat this process for all cells with the probability p_c. As a result, we get a map which is more similar to the small-world network in the Ref. [5]. Figure 3 shows a sketch map of the Rewired SWCNN consisting of 4×4 cells.

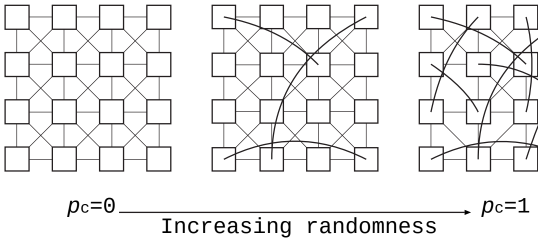

Figure 3: Rewired SWCNN architecture.

The characteristic path length L(p_c) and the clustering coefficient C(p_c) are calculated in Fig. 4. The decrease of the clustering coefficient is quicker than the Added SWCNN. However, the same restriction of the one cell with one short cut makes the difference between the two networks small.

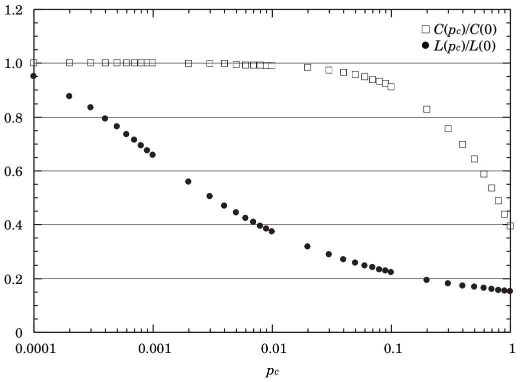

Figure 4: Characteristic path length and clustering coefficient of Rewired SWCNN.

3. APPLYING TO IMAGE PROCESSING

Image processing is one of important applications of the CNN. As well known, many templates and algorithms used for this purpose have been developed. In this section, we investigate the effect of applying the two types of SWCNNs to existing image processing applications.

3.1. Gray-scale edge detection

The edge detection extracts edges of objects in a binary image where each black pixel with at least one white nearest neighbor is defined to be an edge cell. The template (3) is designed to work well for binary input images only.

$$\mathbf{A} = \begin{bmatrix} 0 & 0 & 0 \\ 0 & 1 & 0 \\ 0 & 0 & 0 \end{bmatrix}, \quad \mathbf{B} = \begin{bmatrix} -1 & -1 & -1 \\ -1 & 8 & -1 \\ -1 & -1 & -1 \end{bmatrix}, \quad I = -1. \tag{3}$$

If the input image is a gray-scale image, the output may not be a binary image, and will in general be gray-scale where black pixels correspond to sharp edges, near-black pixels correspond to fuzzy edges, and near-white pixels correspond to noise. The simulation result is shown in Fig. 5. Figure 5(a) is the input gray-scale image. Figure 5(b) is the output image obtained by the original CNN. We apply the same input image to the SWCNN with different random coupling probabilities. Under the above template (3) and the random coupling weight $w_c = -0.5$, the simulation results are shown in Figs. 5(c) and (d), which correspond to the coupling probabilities $p_c = 0.5$ and 1.0, respectively. Note that the Added SWCNN and the Rewired SWCNN give the same output image for this task, because the **A** template has the non-zero value only in the center.

We observe from the simulations that the SWCNN can detect some edges such as the pillar in the left hand side of the image, the pattern of the hat, the face characters, etc. that can not be detected by the original CNN by using the SWCNN. Moreover, the ability of the edge detection become higher with the probability increases. Therefore, we can conclude from these simulation results that the application of the SWCNN to the gray-scale edge detection problem could improve the efficiency of the original CNN.

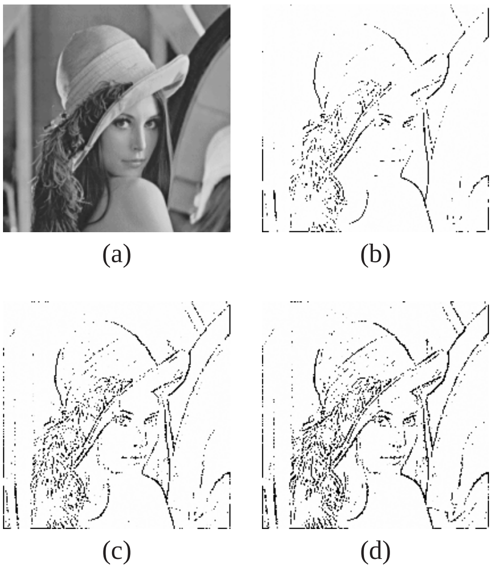

Figure 5: Gray-scale edge detection. (a) Input and initial state image. (b) Output image by the original CNN. (c)-(d) Output images by SWCNN with $p = 0.5$ and 1.0.

3.2. Hole-filling

Hole-filling is defined as filling the interior of all closed contours in a binary image. This temple is shown as follows.

$$\mathbf{A} = \begin{bmatrix} 0 & 1 & 0 \\ 1 & 3 & 1 \\ 0 & 1 & 0 \end{bmatrix}, \quad \mathbf{B} = \begin{bmatrix} 0 & 0 & 0 \\ 0 & 4 & 0 \\ 0 & 0 & 0 \end{bmatrix}, \quad I = -1. \tag{4}$$

This is a propagating template, the computing time is proportional to the length of the image.

Simulated results are shown in Figs. 6 and 7. For this task, the original CNN and the Added SWCNN work well as Fig. 6. However, the Rewired SWCNN can not work as Fig. 7 because of the lack of the designed template values.

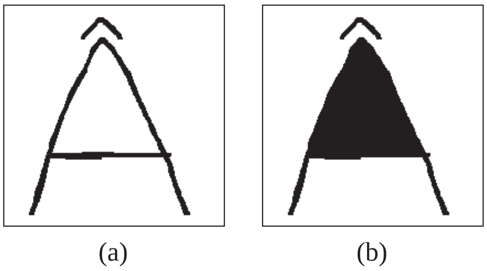

Figure 6: Hole-filling by original CNN and Added SWCNN. (a) Input image. (b) Output image.

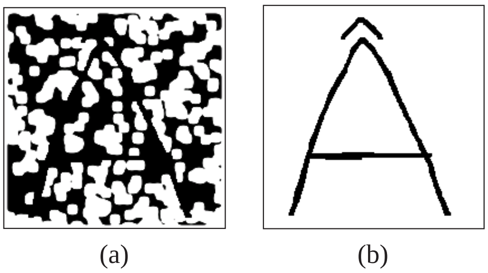

Figure 7: Hole-filling by Rewired SWCNN with p_c=0.01 and w_c=-0.9. (a) Output image after 5 sec. (b) Output image after convergence.

In order to evaluate the ability of the SWCNN, we investigated the convergence speed of the CNNs for this task. The result is shown in Fig. 8. From the figure, we can say that the Added SWCNN converges more quicker than the original CNN. The behavior of the Rewired SWCNN is different from the others, because the network settles down to the different output.

3.3. Smoothing with binary output

The output image obtained by this template is a binary image where black (white) pixels correspond to the locations in an initial state image where the average of pixels intensities

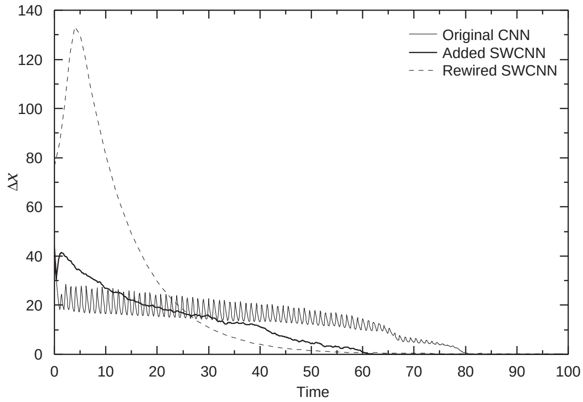

Figure 8: Convergence speed of the three CNNs (p_c=1.0, w_c=-0.9).

over the r=1 feedback convolution window is positive (negative).

$$\mathbf{A} = \begin{bmatrix} 0 & 1 & 0 \\ 1 & 2 & 1 \\ 0 & 1 & 0 \end{bmatrix}, \quad \mathbf{B} = \begin{bmatrix} 0 & 0 & 0 \\ 0 & 0 & 0 \\ 0 & 0 & 0 \end{bmatrix}, \quad I = 0. \tag{5}$$

We carried out computer simulations of the three CNNs with this template. Figure 9(a) shows the input image and 9(b) shows the output image by the orignal CNN. Figure 10 shows the outputs obtained by the Added SWCNN with different p_c. Figure 11 shows the outputs obtained by the Rewired SWCNN with different p_c. We can observe that the Added SWCNN works similarly to the original CNN but the outputs of the Rewired SWCNN look like the images obtained by different templates.

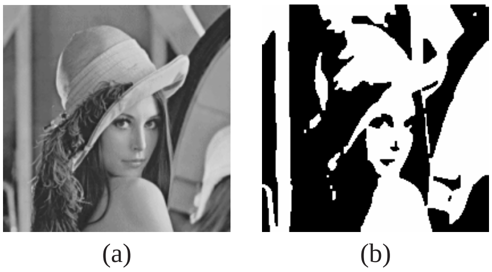

Figure 9: Smoothing by original CNN. (a) Input image. (b) Output image.

4. CONCLUSIONS

In this article, we have proposed two types of network topologies of the SWCNN and investigate the features of the two SWCNNs. We have applied the two SWCNN to several basic image processings. Because we used the templates designed for the original CNN, the obtained outputs were not sufficient for the tasks. However, we confirmed that the SWCNN could improve the convergence speed and could achieve the different image processing tasks.

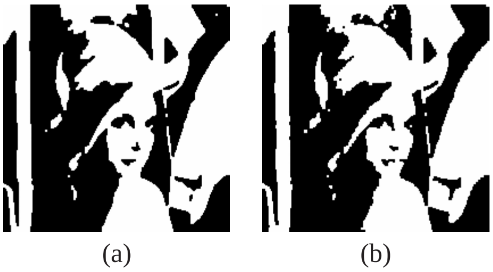

Figure 10: Smoothing by Added SWCNN. (a) p_c=0.1 and w_c=0.5. (b) p_c=1.0 and $w_c = 0.5$.

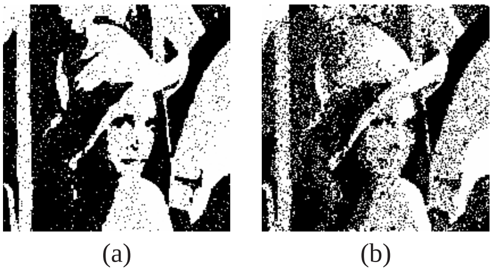

Figure 11: Smoothing by Rewired SWCNN. (a) p_c=0.1 and w_c=0.5. (b) p_c=0.5 and $w_c = 0.5$.

Our important future researchs are design of the template for the SWCNN, investigations of the convergence speed of the SWCNN, and analysis of the stability of the SWCNN.

References

[1] L.O. Chua and L. Yang, "Cellular neural networks: theory and applications," IEEE Trans. Circuits & Syst., vol.35 pp.1257-1290, Oct. 1988.

[2] L.O. Chua and T. Roska, "The CNN paradigm," IEEE Trans. Circuits & Syst., vol.40, pp.147-156, Mar. 1993.

[3] T. Roska, L. Kék, L. Nemes, A. Zarandy and P. Szolgay "CNN software LIBRARY: templates and algorithms", Version7.3, Analogical and Neural Computing Laboratory, Computer and Automation Institute, Hungarian Academy of Sciences, 1999.

[4] Z. Yang, Y. Nishio and A. Ushida, "Image processing of two-layer CNNs – applications and their stability –," IEICE Trans. Fundamentals, vol.E85-A, no.9, pp.2052-2060, Sep. 2002.

[5] D.J. Watts and S.H. Strogatz, "Collective dynamics of small-world networks", Nature 393, pp.440-442, 1998.

[6] K. Tsuruta, Z. Yang, Y. Nishio and A. Ushida, "Small-world cellular neural networks for image processing applications," Proceedings of ECCTD'03, vol.1, pp.225-228, Sep. 2003.